



Preparation and Characterization of $\text{Eu}_{1/2}\text{Ca}_{1/2}\text{Fe}_{1/3}\text{Mn}_{2/3}\text{O}_3$ by Sol-Gel Process†

HUIQIONG NI¹, QI MAO¹ and YONGLI WANG^{2,*}

¹School of Chemical Engineering, Anhui University of Science and Technology, Huainan 232001, Anhui Province, P.R. China

²Department of Physics, Huai Nan Normal University, Huainan 232001, Anhui Province, P.R. China

*Corresponding author: Fax: +86 13695547092; E-mail: hnwangyl@126.com

Published online: 1 March 2014;

AJC-14743

In this paper, crystal of $\text{Eu}_x\text{Ca}_{1-x}\text{Fe}_y\text{Mn}_{1-y}\text{O}_3$ ($1/4 \leq x \leq 1/2$, $1/4 \leq y \leq 1/2$) has been synthesized with sol-gel method, in which gel is sintered in 750 °C with muffle furnace and then grounded into powders. The structure of the synthesized $\text{Eu}_x\text{Ca}_{1-x}\text{Fe}_y\text{Mn}_{1-y}\text{O}_3$ has been studied using X-ray powder diffraction and the results reveal that $\text{Eu}_{1/2}\text{Ca}_{1/2}\text{Fe}_{1/3}\text{Mn}_{2/3}\text{O}_3$ is well-crystallized. The scanning electron microscope demonstrates that $\text{Eu}_{1/2}\text{Ca}_{1/2}\text{Fe}_{1/3}\text{Mn}_{2/3}\text{O}_3$ has a similar layer structure and laser particle size analyzer indicates that the particle size is in the range of 0.5-2.5 μm . The thermogravimetric analysis of $\text{Eu}_{1/2}\text{Ca}_{1/2}\text{Fe}_{1/3}\text{Mn}_{2/3}\text{O}_3$ shows that the material possesses a good thermal stability from 0-900 °C. The electrical property of $\text{Eu}_{1/2}\text{Ca}_{1/2}\text{Fe}_{1/3}\text{Mn}_{2/3}\text{O}_3$ has been analyzed with resistance-temperature curve, which suggests that it is an insulator below 300 K.

Keywords: Sol-gel method, Middle temperature sintering, Iron calcium manganese and europium.

INTRODUCTION

In recent decades, increasing attention has been shifted to ferroelectric materials, ferromagnetic materials and magnetoelectric composites which have broad application prospects in memory industry, microelectronics and computer fields¹⁻³. At the moment, the rare earth-doped calcium manganese perovskites have attracted much attention due to their exotic behaviors, such as pyroelectric effect, magnetic effect⁴. It has been modified that rare earth doped manganese oxides possess Giant Magneto-Resistive (CMR) effects, nanomaterials doped with rare earth ions can be used for preparation of ferromagnetic nanocomposites^{5,6}.

In this paper, we adopted sol-gel method to synthesize gel of Eu, Ca, Mn and Fe compound which was sintered in middle temperature using muffle furnace and then grounded into powder. It is not only simple to operate but also of a low cost to synthesize^{7,8}. Furthermore, in this study we used X-ray powder diffraction (XRD), thermogravimetric analysis (TG), scanning electron microscope (SEM), laser particle size analyzer and the temperature dependence of resistance (R-T curve) to investigate the chemical structure, appearance (or microstructure) and electrical property of the grounded powder. Our results can be referenced to assess the possibility of the $\text{Eu}_{1/2}\text{Ca}_{1/2}\text{Fe}_{1/3}\text{Mn}_{2/3}\text{O}_3$ compound with a good thermal stability

and insulator utilized as potential material for applications of electronics and composite materials⁹.

EXPERIMENTAL

Synthesis of $\text{Eu}_x\text{Ca}_{1-x}\text{Fe}_y\text{Mn}_{1-y}\text{O}_3$ was carried out according to sol-gel method. First of all, some calcium carbonate (CaCO_3), iron nitrate nonahydrate [$\text{Fe}(\text{NO}_3)_3 \cdot 9\text{H}_2\text{O}$], europium oxide (Eu_2O_3) and manganese acetate [$\text{Mn}(\text{CH}_3\text{COO})_2 \cdot 4\text{H}_2\text{O}$] were put in the beaker. Then adding of some ethylenediamine tetraacetic acid (EDTA) and dilute nitric acid, at the same time the solution was stirred at room temperature for 4 h. Subsequently, ethylenediamine ($\text{H}_2\text{NCH}_2\text{CH}_2\text{NH}_2$) was slowly added to the solution to make it neutral and finally the sol was obtained. The above sol continued being stirred for 4 h in order to get uniform gel. Then the gel was transferred to a crucible and dried in an oven. After the gel was dried, it was transferred to a muffle furnace and calcined. When the temperature of muffle furnace increased to 160 °C, heating was continued for 4 h so as to decompose organic matter. The temperature was then increased to 750 °C and kept for 8 h. Then the product was natural cooled to room temperature and grounded into powders in an agate mortar. Finally the powders were put into muffle furnace to calcined for another 4 h and then cooled and removed out to study their properties.

†Presented at The 7th International Conference on Multi-functional Materials and Applications, held on 22-24 November 2013, Anhui University of Science & Technology, Huainan, Anhui Province, P.R. China

The phase purity and composition of the $\text{Eu}_x\text{Ca}_{1-x}\text{Fe}_y\text{Mn}_{1-y}\text{O}_3$ were checked by X-ray diffraction (XRD, XD-3, Beijing). The micro-structural morphology and size of $\text{Eu}_{1/2}\text{Ca}_{1/2}\text{Fe}_{1/3}\text{Mn}_{2/3}\text{O}_3$ were observed using scanning electron microscope (SEM, S-4800IIIFESM, Japan) and a BT-9300H laser particle size analyzer. Thermogravimetric analysis (TG, STA409PC, Germany) was performed under Nitrogen atmosphere with a heating/cooling rate of 10 °C/min. The temperature dependence of resistance (resistance vs. temperature curve) was measured from 25-280 K using the standard four-probe method¹⁰.

RESULTS AND DISCUSSION

Structural character of $\text{Eu}_x\text{Ca}_{1-x}\text{Fe}_y\text{Mn}_{1-y}\text{O}_3$: Fig. 1 shows the XRD patterns of $\text{Eu}_x\text{Ca}_{1-x}\text{Fe}_y\text{Mn}_{1-y}\text{O}_3$. With the change in concentration of x and y, the position of the peak shows no apparent shift in each sample. However, it is not sure that there is no distortion for the crystal lattice structure. As expected, several sharp peaks have been observed from XRD patterns in different samples, but the sharp peaks of $\text{Eu}_{1/2}\text{Ca}_{1/2}\text{Fe}_{1/3}\text{Mn}_{2/3}\text{O}_3$ are higher than those of other samples which indicates that the $\text{Eu}_{1/2}\text{Ca}_{1/2}\text{Fe}_{1/3}\text{Mn}_{2/3}\text{O}_3$ is well-crystallized.

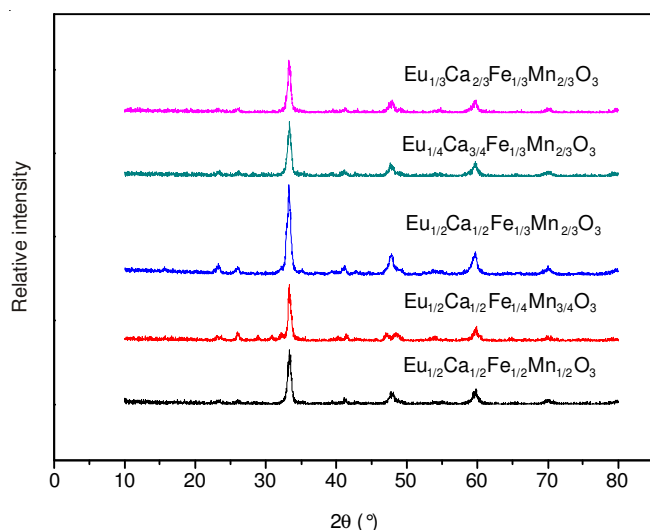


Fig. 1. XRD spectra of $\text{Eu}_x\text{Ca}_{1-x}\text{Fe}_y\text{Mn}_{1-y}\text{O}_3$

It can also be observed from the comparison of the standard XRD patterns of Eu_2O_3 and CaMnO_3 that there is no strong absorption at 28.45 and 33.98°, indicating that no Eu_2O_3 and CaMnO_3 exist in the sample powders, the differences only exist in peak position. According to the peak position and Bragg formula, the value of each d can be calculated and the crystal indices are corresponding with the XRD patterns of CaMnO_3 , illustrating that $\text{Eu}_{1/2}\text{Ca}_{1/2}\text{Fe}_{1/3}\text{Mn}_{2/3}\text{O}_3$ is the type of ABO_3 . Compared with other groups of XRD patterns, the peak position of $\text{Eu}_{1/2}\text{Ca}_{1/2}\text{Fe}_{1/3}\text{Mn}_{2/3}\text{O}_3$ is closer to the standard patterns, with sharper peak and almost no impurity peaks. All these observations suggest that $\text{Eu}_{1/2}\text{Ca}_{1/2}\text{Fe}_{1/3}\text{Mn}_{2/3}\text{O}_3$ crystal structure has been formed correctly, Eu and Fe are well-doped. In the following characterization part, all samples used are $\text{Eu}_{1/2}\text{Ca}_{1/2}\text{Fe}_{1/3}\text{Mn}_{2/3}\text{O}_3$, which means Eu has been doped well in CaMnO_3 structure.

SEM and size of $\text{Eu}_{1/2}\text{Ca}_{1/2}\text{Fe}_{1/3}\text{Mn}_{2/3}\text{O}_3$: Scanning electron microscopy (SEM) images and size distribution of $\text{Eu}_{1/2}\text{Ca}_{1/2}\text{Fe}_{1/3}\text{Mn}_{2/3}\text{O}_3$ powders are displayed in Figs. 2 and 3, respectively. It shows that the $\text{Eu}_{1/2}\text{Ca}_{1/2}\text{Fe}_{1/3}\text{Mn}_{2/3}\text{O}_3$ powder has a similar layer structure which can be described as agglomeration. Size distribution of powders shows a relatively uniform grain size distribution, indicating that sol-gel process is a good method to prepare powders with uniform features. The powders exhibit a relatively regular shape and an inhomogeneous size distribution is due to the crystallite growth at high temperature. As shown in Fig. 3, the particle size of $\text{Eu}_{1/2}\text{Ca}_{1/2}\text{Fe}_{1/3}\text{Mn}_{2/3}\text{O}_3$ is in the range of 0.5-2.5 μm.

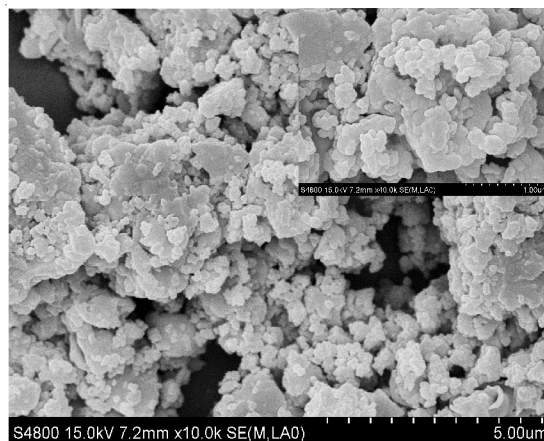


Fig. 2. SEM images of $\text{Eu}_{1/2}\text{Ca}_{1/2}\text{Fe}_{1/3}\text{Mn}_{2/3}\text{O}_3$, the inset image was partial enlarged view

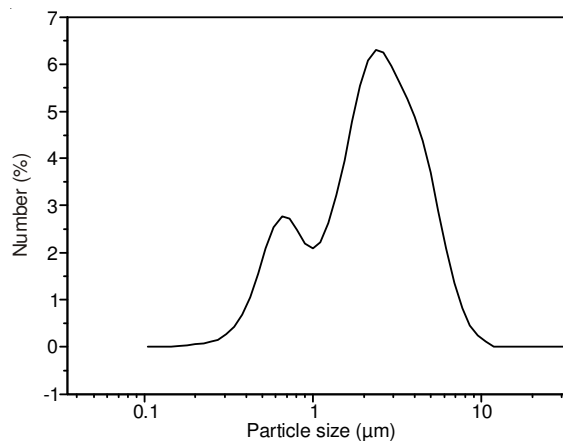


Fig. 3. Size distribution of $\text{Eu}_{1/2}\text{Ca}_{1/2}\text{Fe}_{1/3}\text{Mn}_{2/3}\text{O}_3$

Thermogravimetric analysis of $\text{Eu}_{1/2}\text{Ca}_{1/2}\text{Fe}_{1/3}\text{Mn}_{2/3}\text{O}_3$:

Fig. 4 shows the TG analysis curve of $\text{Eu}_{1/2}\text{Ca}_{1/2}\text{Fe}_{1/3}\text{Mn}_{2/3}\text{O}_3$. As shown in Fig. 4, there are three stages in the weight loss process. The first stage region belongs to the loss of combined water of $\text{Eu}_{1/2}\text{Ca}_{1/2}\text{Fe}_{1/3}\text{Mn}_{2/3}\text{O}_3$, from 29-105 °C and the ratio of weight loss is 0.2173 %. The second stage is from 105-442 °C, the weight loss of $\text{Eu}_{1/2}\text{Ca}_{1/2}\text{Fe}_{1/3}\text{Mn}_{2/3}\text{O}_3$ should be a small amount of the remaining organic matters decomposition and the ratio of weight loss is 0.5651 %. The ratio of weight loss of the third stage is 1.0012 %. Total ratio of weight loss of all the three stages is 1.7863 %, so the weight loss in the whole temperature range is very small which indicates that the material possesses a good thermal stability.

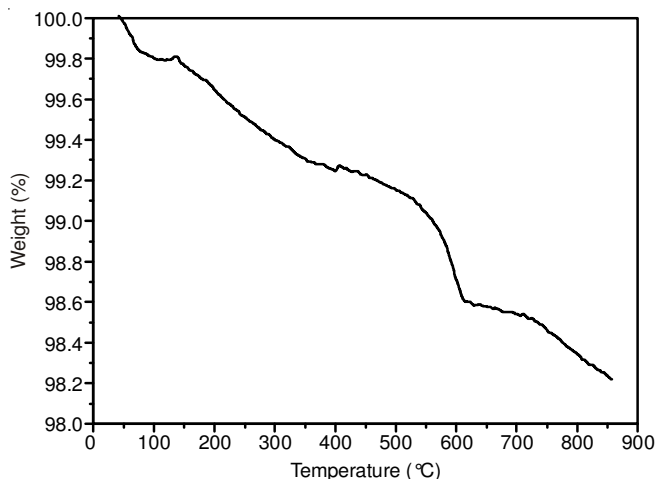


Fig. 4. TG analysis curve of $\text{Eu}_{1/2}\text{Ca}_{1/2}\text{Fe}_{1/3}\text{Mn}_{2/3}\text{O}_3$

Temperature dependence of the electrical resistance of $\text{Eu}_{1/2}\text{Ca}_{1/2}\text{Fe}_{1/3}\text{Mn}_{2/3}\text{O}_3$: Fig. 5 shows the temperature dependence of electrical resistance of $\text{Eu}_{1/2}\text{Ca}_{1/2}\text{Fe}_{1/3}\text{Mn}_{2/3}\text{O}_3$, which was measured in the range of 80-300 K using the standard four-probe method. It can be noticed that the resistance of the sample decreases with the increase of temperature. The tiny change at 149 K is caused by the large contact resistance in the experimental process, rather than phase change process. From the graph (Fig. 5) we can also see that the resistance as well as the resistivity of the sample keeps increasing with the decrease of the temperature. When the temperature reduces less than 110 K, the increase of resistance is not obvious. There is no phase change on sample from insulator to metal (I-M) during the resistance measurement process, explaining that the sample is an insulator.

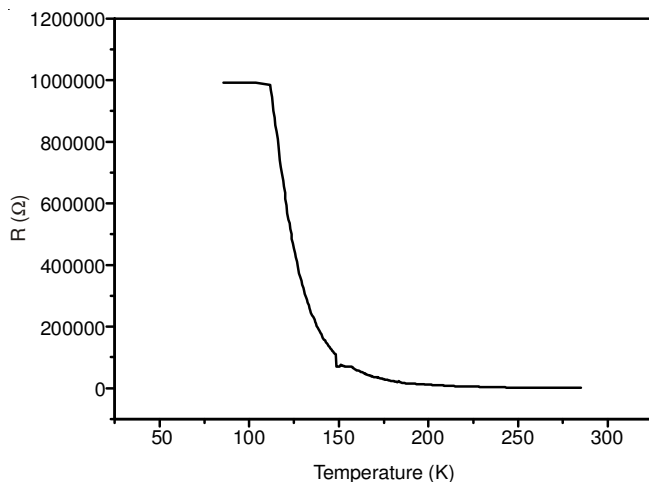


Fig. 5. R-T curve of $\text{Eu}_{1/2}\text{Ca}_{1/2}\text{Fe}_{1/3}\text{Mn}_{2/3}\text{O}_3$

Conclusion

In this paper, we studied the synthesis, structure, morphology, size and temperature dependence of resistance of $\text{Eu}_{1/2}\text{Ca}_{1/2}\text{Fe}_{1/3}\text{Mn}_{2/3}\text{O}_3$. The best molar ratio of starting material is $n\text{Eu}_2\text{O}_3:n\text{CaCO}_3:n\text{Fe}(\text{NO}_3)_3 \cdot 9\text{H}_2\text{O}:n\text{Mn}(\text{CH}_3\text{COO})_4 = 3:6:4:8$ and an insulator were prepared with this ratio. The results showed that $\text{Eu}_{1/2}\text{Ca}_{1/2}\text{Fe}_{1/3}\text{Mn}_{2/3}\text{O}_3$ powders produced with sol-gel method were well-structured, powders with similar layered structure and the particle size in the range of 0.5-2.5 microns. Moreover, this novel $\text{Eu}_{1/2}\text{Ca}_{1/2}\text{Fe}_{1/3}\text{Mn}_{2/3}\text{O}_3$ compound is expected to be used as potential materials for electronics and composite materials and the further studies are underway.

ACKNOWLEDGEMENTS

Project supported by the Education Office of Anhui Province of China (Grant No. KJ2010B448).

REFERENCES

1. R. Haumont, R. Saint-Martin and C. Byl, *Phase Transit.*, **81**, 881 (2008).
2. Y.Z. Cao, J.-H. He, Z.H. Liu, Y. Mei, B.Q. Liu, X. Lin and Z.-A. Xu, *Chinese J. Low Temp. Phys.*, **32**, 337 (2010).
3. S.N. Tie, X. Li and Y.J. Li, *China Powder Sci. Technol.*, **15**, 68 (2009).
4. N.H. Linh, N.T. Trang, N.T. Cuong, P.H. Thao and B.T. Cong, *Comput. Mater. Sci.*, **50**, 2 (2010).
5. N. Liu, S.J. Xu, H.Y. Guo, W. Tong and Y.-H. Zhang, *Acta Phys. Sin.*, **54**, 912 (2005).
6. F.P. Zhang, X. Zhang, Q.M. Lu, Y.-Q. Liu and J.-X. Zhang, *Acta Phys. Sin.*, **60**, 087205 (2011).
7. B. Liu, T. Sun, J.Q. He and V.P. Dravid, *ACS Nano*, **4**, 6836 (2010).
8. L.S. Fu, H.J. Zhang, H. Shao *et al.*, *Mater. Sci. Eng.*, **17**, 84 (1999).
9. M. Anwar-ul-Haq, S. Barsanti, A. Bogi and P. Bicchì, *Opt. Mater.*, **31**, 1860 (2009).
10. X.W. Dong, K.F. Wang, J.G. Wan, J.S. Zhu and J.-M. Liu, *J. Appl. Phys.*, **103**, 94101 (2008).